Progress of Theoretical Physics, Vol. 98, No. 3, September 1997

# Thermodynamical Properties of Asymmetric Nuclear Matter in Generalized Hybrid Derivative Coupling Model

Binay MALAKAR and Sasabindu SARKAR

*Department of Theoretical Physics*
*Indian Association for the Cultivation of Science, Jadavpur, Calcutta-700032*

(Received August 26, 1996)

In this work we have studied the properties of asymmetric nuclear matter at zero and finite temperature in a wide range of density and asymmetry parameter using recently proposed generalized hybrid derivative coupling model. The temperature and asymmetry dependence of the bulk quantities such as compressibility, binding energy per nucleon, saturation density, chemical potential, entropy per nucleon, etc. have been explored. This is useful to understand the dynamics of supernova explosion. We have studied the density and temperature dependence of symmetry energy and briefly discussed its role in the evaluation of proton fraction at $T = 0$, in equilibrium with neutron rich matter. We have also studied proton fraction for $T \neq 0$ by free energy minimization. Dependence of bulk properties on the hybridization parameter of our model has been studied. The asymmetry and temperature dependence of the characteristics of liquid-gas phase transition have also been studied. We have compared our results with those of other investigators.

## §1. Introduction

The study of the properties of cold and hot asymmetric nuclear matter is very important to understand the dynamics of iron-core collapse of some massive stars which produce type II supernova, the mechanism of supernova explosion, the structure of neutron-star remnants and also unstable neutron rich nuclei produced in the laboratory.[1] For this purpose we need an equation of state (EOS) which is reliable at high density and/or non-zero temperature. The later stage of the collapsing presupernova core involves neutron rich matter with $N \cong 2Z$ (or proton concentration $(Z/(N+Z)$ of about 1/3) at moderate temperature $T = 1 - 10$ MeV and densities up to about $4\rho_0$[2] where $\rho_0$ is the saturation density of nuclear matter. Neutron star structure involves almost pure neutron matter with $N \gg Z$, essentially at zero temperature and densities up to about $(8-10)\rho_0$.[2]

The problem of asymmetric nuclear matter for zero and non-zero temperature has been investigated by several investigators who used non-relativistic Brueckner-Bethe-Goldstone approach.[2],[3] They assumed potential theory description. In this problem several workers[4] have performed relativistic Dirac-Brueckner calculations, based on a one-meson exchange interaction only. Prakash and Ainsworth[5] applied field theoretic method based on chiral sigma model to study asymmetric nuclear matter properties at zero temperature. We intend to study the properties of asymmetric nuclear matter using a recently proposed general form of hybrid derivative coupling model[6] considering different values of asymmetric parameter $\beta(= (N-Z)/(N+Z))$ and hybridization parameter $\alpha$. It may be noted that several investigators[7] have studied certain aspects of asymmetric nuclear matter and neutron matter using derivative coupling model[8] of Zimanyi and Moszkowski which is a particular case of our hybrid derivative coupling model.[6] We may further note that Delfino et al.[9] and Miyazaki[10] have proposed modified and generalized form of the Zimanyi and Moszkowski model. In the present model the strength of the Yukawa point coupling and that of the derivative coupling of scalar mesons to nucleons is taken in the ratio $(1-\alpha)/\alpha$. In pure derivative scalar coupling (DSC) model[8] the scalar meson ($\sigma$) couples only to the derivative of the nucleon wave function ($\psi$) and to the iso-scalar vector meson ($\omega_\mu$), in contrast to Walecka's model[11] in which the scalar mesons have the Yukawa point coupling to the nucleons. Further modification of the DSC model[8] was done by Glendenning et al.[12] who used a particular form of hybrid derivative coupling in which a scalar meson couples equally (with equal strength) to both the baryon wave function and its derivative.

It may be noted that a soft EOS is needed to understand the explosion mechanism of a type II supernova.[13] On the other hand, a quite stiff EOS is favored by the systematic analysis of the observed masses of neutron star.[14] In this connection Nishizaki et al.[15] observed that such a 'conflicting constraint' arising from maximum neutron star mass and supernova explosion can be resolved by considering asymmetry and temperature dependence of compressibility $K$. This dependence of $K$ on asymmetry parameter $\beta$ and temperature $T$ has been studied in this paper. In the present hybrid derivative coupling model we can have a soft or a stiff EOS depending upon the value of the hybridization parameter $\alpha$.[6]

The present work is just an extension of our previous work[6] on symmetric nuclear matter by including the contribution of $\rho$-meson. The effect of temperature is also considered in this paper. Several investigators[16] have remarked that the properties of asymmetric nuclear matter for any arbitrary value of $\beta$ can be extracted by interpolation method from the corresponding findings for symmetric nuclear matter ($\beta = 0$) and neutron matter ($\beta = 1$) with the help of parabolic approximation. We have somewhat verified the empirical parabolic law[16] (involving $\beta^2$ term) satisfied by the binding energy per nucleon in all the range of the asymmetry parameter $\beta$ for different baryon densities at zero and non-zero temperature in our model. However, theoretical analysis shows a small $\beta^4$ dependence besides the $\beta^2$ dependence of the binding energy of the asymmetric nuclear matter. It may be noted that the symmetry energy, related to the binding energy of asymmetric system, determines the amount of conversion of neutrons to protons and leptons near the top of the Fermi sea[5] at zero temperature. For $T \neq 0$, proton fraction has been studied by minimizing the free energy.

Liquid gas phase transition is one of the striking features of nuclear matter at subnuclear density. The characteristics of liquid-gas phase transition, such as critical temperature $T_c$ and critical density $\rho_c$, are found to depend on the value of asymmetry parameter ($\beta$) and hybridization parameter ($\alpha$). The dependence of isothermal bulk modulus, specific heat, effective mass and neutron and proton chemical potentials on asymmetry parameter $\beta$ , temperature $T$ and also on hybridization parameter $\alpha$ have been investigated. We have determined the value of $\beta$ and the corresponding density at which both pressure and compressibility vanish. Further, the values of $\beta$ and density for which binding energy and pressure simultaneously become zero have also been evaluated. It may be mentioned that satisfactory values of bulk properties of nuclear matter can be obtained by choosing a suitable value of the hybridization parameter $\alpha$ which is found to be about 1/4 in our model.[6] We have calculated the entropy per nucleon $(s/\rho)$ in our model for $\alpha = \frac{1}{4}$ and compared it with the experimental values.[17] The isoentropic bulk modulus $(K_s)$ as a function of entropy has been calculated. The dependence of symmetry energy on density and temperature has also been studied.

It may be noted that several investigators[18] have used the variational method to study the correlation effect in the framework of potential theory formalism. They have considered correlation induced by two nucleon potential. Serot and Walecka,[11] Brittan[19] and Boguta and Bodmar[20] have observed that compressibility $(K)$ can be reduced by two body correlation or by explicit introduction of nonlinear nucleon meson couplings. In our hybrid model equivalent form of the field theoretic Lagrangian contains the feature of nonlinear interaction term involving scalar meson field and nucleon wave function. This feature of our model like correlation reduces the compressibility which is quite large in the Walecka Model.[11] In the renormalizable Walecka model it is found that the scalar meson exchange energy[21] $\epsilon^s_{\rm ex} = \frac{1}{4}(\frac{1}{2\pi})^4 g_s k_F^4$ (where $g_s$ is the scalar meson nucleon coupling constant and $k_F$ is the Fermi momentum) and there is a similar expression for vector meson exchange energy. The mean field theory energy is proportional to $k_F^6$. This implies[21] that exchange energy corrections are not important in the high density region in which we are interested. The relativistic DSC model[8] and the other related models[9),10] including the present one[6] are not renormalizable. In this connection Glendening et al.[12] observed that since nuclear field theory is an effective one, this is not a 'weighty objection'. In the mean field theory calculation the parameters of our nonlinear model are chosen to reproduce the bulk properties of nuclear matter and thus to some extent take into account higher order 'corrections' to direct energy part like exchange energy and correlation effect specially in the region around saturation density. Further these corrections are negligible for highly dense nuclear matter.

The parameters of field theoretic model which are applied to determine the EOS of nuclear matter and also properties of finite nuclei, are obtained from the bulk properties of nuclear matter. So it is natural to expect that our model giving reasonable values for properties of nuclear matter, is likely to give satisfactory values for the properties of finite nuclei. It may be noted that recently Delfino et al.[9] and Miyazaki[10] have used extended versions of the DSC model to study only infinite nuclear matter. The purely derivative scalar coupling (DSC) model of Zimanyi and Moszkowski $(\alpha = 1)$ has already been used to study finite nuclei.[22),23] In our previous paper[6] it has already been discussed that we may obtain better result for spin orbit splitting in our hybrid model (for $\alpha \cong \frac{1}{4}$) than that in the DSC model. We intend to apply our hybrid model (an extension of the DSC model) to study finite nuclei in a later paper. The relativistic $\rho$-meson-nucleon coupling used in this paper for asymmetric nuclear matter $(N \neq Z)$ is the same as applied by other recent investigators. Some nonrelativistic interaction potential used to study unstable finite nuclei $(N \neq Z)$ may not give a satisfactory result for the properties of highly dense and hot asymmetric nuclear matter in which we are interested in this paper.

This paper is organized as follows. In §2 we give a brief description of our model. In §3 we give the results of our calculation and the comparison of our results with other recent findings. Section 4 contains a summary of our work.

## §2. General form of hybrid derivative scalar coupling model to study asymmetric nuclear matter

The details of the general form of the hybrid derivative coupling model have already been given in our earlier publication.[6)] We give here a brief description of the above model for asymmetric nuclear matter where additional contribution due to isovector-vector meson is to be considered. We consider the following form of Lagrangian for asymmetric nuclear matter

$$L = \left(1+\alpha\frac{\sigma g_s}{M}\right)\overline{\psi}\left(i\gamma^\mu\theta_\mu - g_v\gamma^\mu\omega_\mu - \frac{1}{2}g_\rho\gamma^\mu\tau\cdot\rho_\mu\right)\psi - \left[1-(1-\alpha)\frac{\sigma g_s}{M}\right]M\overline{\psi}\psi$$
$$+\frac{1}{2}\left(\partial^\mu\sigma\theta_\mu\sigma - m_s^2\sigma^2\right) - \frac{1}{4}\omega^{\mu\nu}\omega_{\mu\nu} + \frac{1}{2}m_v^2\omega^\mu\omega_\mu - \frac{1}{4}\rho^{\mu\nu}\cdot\rho_{\mu\nu} + \frac{1}{2}m_\rho^2\rho^\mu\cdot\rho_\mu, \quad (1)$$

where $\psi$ denotes a baryon (neutron and proton) wave function of mass $M$. $\sigma$, $\omega^\mu$ and $\rho^\mu$ are iso-scalar scalar, iso-scalar vector and iso-vector vector meson fields with masses $m_s$, $m_v$ and $m_\rho$, respectively. The quantities $\omega^{\mu\nu}$ and $\rho^{\mu\nu}$ are the antisymmetric field tensors for $\omega$- and $\rho$-mesons. The $\rho$-meson coupling constant $g_\rho$ is adjusted to give the empirical symmetry energy coefficient. Equation (1) implies that the ratio of the strength of Yukawa point coupling and that of the derivative coupling is given by $(1-\alpha)/\alpha$. A suitable value of $\alpha$ may be chosen which gives satisfactory results for bulk properties of nuclear matter. It is also evident from the relation (1) that there is coupling between scalar meson and vector meson. We have used the notation and convention of Refs. 6), 8), 11) and 12). It is convenient to work with the following transformed Lagrangian,[6)]

$$L = \overline{\psi}\left(i\gamma^\mu\partial_\mu - M^* - g_v\gamma^\mu\omega_\mu - \frac{1}{2}g_\rho\gamma^\mu\tau\cdot\rho_\mu\right)\psi$$
$$+\frac{1}{2}\left(\partial^\mu\sigma\partial_\mu\sigma - m_s^2\sigma^2\right) - \frac{1}{4}\omega^{\mu\nu}\omega_{\mu\nu} + \frac{1}{2}m_v^2\omega^\mu\omega_\mu - \frac{1}{4}\rho^{\mu\nu}\cdot\rho_{\mu\nu} + \frac{1}{2}m_\rho^2\rho^\mu\cdot\rho_\mu \quad (2)$$

which is obtained from (1) by rescaling[6)] the baryon wave function

$$\psi \to \psi\left(1+\alpha\frac{\sigma g_s}{M}\right)^{-1/2}. \quad (3)$$

The effective mass $M^*$ occurring in (2) is given by

$$M^* = \frac{1-(1-\alpha)\sigma g_s/M}{1+\alpha\sigma g_s/M}M. \quad (4)$$

The hybridization parameters $\alpha$ = 0.0, 1/2 and 1 correspond to the models of Walecka,[11)] Glenndening et al.,[12)] and Zimanyi and Moszkowski[8)] respectively. In the mean field theory (MFT) approximation the field equations for uniform static nuclear matter are given in the following,

$$\omega_0 = \left(\frac{g_v}{m_v^2}\right) \rho_B, \tag{5}$$

where

$$\rho = \rho_B = \sum_{i=n,p} \rho_i, \tag{6}$$

is the total baryon density and

$$\rho_i = \frac{2}{(2\pi)^3} \left[\int_0^\infty d^3k (n_{ik}(T) - \overline{n}_{ik}(T))\right], \tag{7}$$

where the suffix $i$ refers to either neutron ($n$) or proton ($p$). In Eq. (7) $n_{ik}(T)$ and $\overline{n}_{ik}(T)$ are baryon and anti-baryon thermal distribution functions with

$$n_{ik}(T) = \left[\exp \frac{E_i^*(k) - \nu_i}{T} + 1\right]^{-1}, \tag{8}$$

$$\overline{n}_{ik}(T) = \left[\exp \frac{E_i^*(k) + \nu_i}{T} + 1\right]^{-1}, \tag{9}$$

where

$$E_i^*(k) = \left(k_{Fi}^2 + M^{*2}\right)^{1/2}, \tag{10}$$

and $\nu_i$ is the shifted (or effective) chemical potential. The expectation value of the time like, neutral component of the $\rho_\mu$ field is given by

$$\rho_{03} = \frac{1}{2} \left(g_\rho / m_\rho^2\right) \rho_3, \tag{11}$$

where

$$\rho_3 = \rho_p - \rho_n. \tag{12}$$

The asymmetry parameter $\beta$ is defined as

$$\beta = \frac{\rho_n - \rho_p}{\rho_n + \rho_p} = -\frac{\rho_3}{\rho_B}. \tag{13}$$

The scalar field is given by

$$\sigma = (g_s/m_s^2) \frac{\rho_s}{[1 + \alpha\sigma g_s/M]^2}, \tag{14}$$

where

$$\rho_s = \sum_{i=n,p} \rho_{si}. \tag{15}$$

The scalar density $\rho_{si}$ is expressed as

$$\rho_{si} = \frac{2}{(2\pi)^3} \int_0^\infty d^3k \frac{M^*}{(k^2 + M^{*2})^{\frac{1}{2}}} (n_{ik}(T) + \overline{n}_{ik}(T)). \tag{16}$$

Combining Eqs. (4) and (13) we obtain the expression for dimensionless effective mass

$$\tilde{M}^* = \frac{M^*}{M} = 1 - \frac{C_s^2}{M^3}\left[1 - \alpha(1 - \tilde{M}^*)\right]^3 \rho_s. \tag{17}$$

Using standard procedure we obtain the following expression for the total energy density,

$$\epsilon = \epsilon_\omega + \epsilon_\rho + \epsilon_\sigma + \frac{2}{(2\pi)^3}\sum_{i=n,p}\int_0^\infty d^3k(k^2 + M^{*2})^{\frac{1}{2}}\left[n_{ik}(T) + \bar{n}_{ik}(T)\right] \tag{18}$$

and pressure

$$P = \epsilon_\omega + \epsilon_\rho - \epsilon_\sigma + \frac{1}{3}\frac{2}{(2\pi)^3}\sum_{i=n,p}\int_0^\infty d^3k \frac{k^2}{(k^2 + M^{*2})^{\frac{1}{2}}}\left[n_{ik}(T) + \bar{n}_{ik}(T)\right], \tag{19}$$

where

$$\epsilon_\omega + \epsilon_\rho = \frac{1}{2}C_v^2\frac{\rho_B^2}{M^2} + \frac{1}{8}C_\rho^2\frac{\rho_3^2}{M^2} \tag{20}$$

and

$$\epsilon_\sigma = \frac{M^2}{2C_s^2}\frac{(M - M^*)^2}{\left[(1 - \alpha(1 - \tilde{M}^*)\right]^2}. \tag{21}$$

In Eqs. (17), (20) and (21) we introduce dimensionless quantities given by

$$C_s^2 = \frac{g_s^2 M^2}{m_s^2}, \tag{22}$$

$$C_v^2 = \frac{g_v^2 M^2}{m_v^2} \tag{23}$$

and

$$C_\rho^2 = \frac{g_\rho^2 M^2}{m_\rho^2}. \tag{24}$$

The chemical potentials for neutron ($\mu_n$) and proton ($\mu_p$), at non-zero temperature ($T \neq 0$), are given by

$$\mu_n = \nu_n + g_v\omega_0 - \frac{1}{2}g_\rho\rho_{03}, \tag{25}$$

$$\mu_p = \nu_p + g_v\omega_0 + \frac{1}{2}g_\rho\rho_{03}. \tag{26}$$

At zero temperature ($T = 0$)

$$\nu_i = \left(k_{Fi}^2 + M^{*2}\right)^{1/2}, \quad i = p, n. \tag{27}$$

The entropy per nucleon (dimensionless) at temperature $T$ is given by

$$s/\rho_B = \frac{\epsilon + P - \rho_p\mu_p - \rho_n\mu_n}{T\rho_B}. \tag{28}$$

## §3. Results and discussion

### 3.1. *Variation of energy per nucleon with density, asymmetry parameter and temperature*

Binding energy ($\epsilon/\rho_B - M$) versus $\rho_B/\rho_0$ for $\beta = 0$, 0.3 and 1 at $T = 0$ MeV and 30 MeV are shown in Fig. 1. For $T = 0$ MeV minima of binding energy are $-16$ MeV (occurring at $\rho_B/\rho_0 = 1$) and $-13.47$ MeV (occurring at $\rho_B/\rho_0 = .902$) for $\beta = 0$ and 0.3 respectively. Neutron matter has no negative binding energy at any density even for $T = 0$ MeV. As evident from Fig. 5, the effective mass $M^*$ for neutron matter is greater than that for symmetric nuclear matter and consequently Fermi energy density for neutron matter is greater than that for symmetric system at the same density and temperature. Even without the repulsive contribution of $\rho$-meson to the binding energy it is found that $(\epsilon/\rho - M)$(in MeV) is $-0.0071(\rho_{\rm sat} = 0.569\rho_0)$, $-2.74(\rho_{\rm sat} = 0.602\rho_0)$ and $-3.71(\rho_{\rm sat} = 0.51\rho_0)$ for $\alpha = 0$, 1/4 and 1 respectively. Terms within the bracket refer to the saturation density. Since the repulsive contribution of $\rho$-meson to the binding energy increases as $\beta$ is enhanced, the 'minimum point' of the binding energy moves to the low density region as shown by the above-mentioned data and the curves of Fig. 1. Purely neutron matter is always found to be unbound. Since thermal effect is larger at the lower density, the minimum point generally occurs at higher density[15] with increasing temperature. For symmetric matter ($\beta = 0$) as $T$ is increased the value of $(\rho_B/\rho_0)_{\rm min}$ at which the minimum of $(\epsilon/\rho_B - M)$ occurs, first increases to the value 1.37 (at $T = 77.8$ MeV), then slightly decreases to the value 1.29 (at $T = 120$ MeV) and afterwards continuously increases with temperature. For $T = 30$ MeV the value of $(\rho_B/\rho_0)_{\rm min}$ is 1.27, 1.19 and .558 for $\beta = 0$, 0.3 and 1, respectively. We also find that $(\rho_B/\rho_0)_{\rm min}$ continuously increases with increasing temperature for $\beta = 0.3$ and $\beta = 1$ (neutron matter). For $\beta = 1$, $(\rho_B/\rho_0)_{\rm min}$ does not exist for $T < 3.5$ MeV. In Fig. 1 we assume $\alpha = 1/4$. The binding energy per nucleon defined as

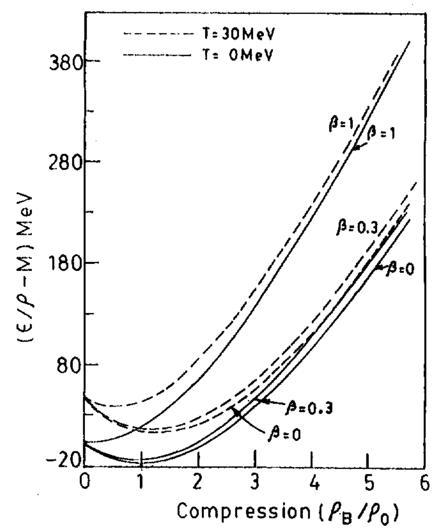


Fig. 1. Variation of binding energy per nucleon with dimensionless density $\rho_B/\rho_0$ for different values of asymmetry parameter $\beta$ and temperature $T$ for the model characterized by hybridization parameter $\alpha = 1/4$.

$$B(\rho_B, T, \beta) - M = \frac{\epsilon(\rho_B, T, \beta)}{\rho_B} - M = E(\rho_B, T, \beta) - M \tag{29}$$

satisfies the following empirical parabolic law[16] for all values of $\beta$ and for densities up to and even greater than $5\rho_0$ and for temperature up to and somewhat greater than 40 MeV.

$$B(\rho_B,T,\beta)=B(\rho_B,T,\beta=0)+E_{\rm sym}(\rho_B,T)\beta^2. \tag{30}$$

In the case when density is not very large, $E_{\rm sym}(\rho_B,T)\beta^2$ ($\beta$ dependent part of energy per nucleon in a field theoretic model), can be expressed as

$$E_{\rm sym}(\rho_B,T)\beta^2 = \frac{1}{8M^2}\beta^2C_\rho^2\rho_B+\frac{1}{6}\left[\beta^2\frac{k_F^2}{(k_F^2+M^{*2})^{1/2}}+\frac{1}{27}\beta^4\frac{k_F^2}{M^*}\left(1+\frac{1}{4}\frac{k_F^2}{M^{*2}}+\cdots\right)+\cdots\right]. \tag{31}$$

The term involving $\beta^4$ in the above relation has not been considered by Prakash and Ainsworth.[5] However, this term is not negligible when $\beta$ is nearly equal to unity. Neglect of $\beta^4$ involving term leads to the above-mentioned empirical parabolic law.[16] The relation (30) has been verified by Bombaci and Lombardo[16] for zero temperature and for several densities. They have used the Brueckner-Bethe-Goldstone

Table I. Dependence of binding energy $B(\rho_0,T=0,\beta)$, saturation density $\rho(T,\beta)$ bulk modulus $K(\rho_B,T,\beta)$ and the parameters $a$ and $b$ on asymmetry parameter $\beta$ at zero temperature for different models.

| Model | $\beta$ | $\frac{\rho_B}{\rho_0}$ | $B(\rho_B,0,\beta)$ (MeV) | $K$ (MeV) | $a$ | $b$ |
|---|---|---|---|---|---|---|
| $\alpha=0.0$ | 0.0 | 1.000 | −16.00 | 548 | 0.68 | 0.60 |
| | 0.4 | 0.904 | −10.91 | 401 | | |
| | 0.8 | 0.547 | +.326 | 88.6 | | |
| | 0.902 | 0.278 | +2.85 | 0 | | |
| $\alpha=0.25$ | 0.0 | 1.000 | −16.00 | 307 | 1.41 | 0.92 |
| | 0.2 | 0.963 | −15.06 | 295 | | |
| | 0.4 | 0.852 | −11.36 | 241 | | |
| | 0.6 | 0.680 | −6.04 | 156 | | |
| | 0.8 | 0.442 | −.363 | 62.7 | | |
| | 0.915 | 0.190 | +2.23 | 0 | | |
| $\alpha=1.0$ | 0.0 | 1.000 | −16.00 | 225 | 1.30 | 1.00 |
| | 0.4 | 0.83 | −11.05 | 177 | | |
| | 0.8 | 0.385 | −.704 | 51.5 | | |
| | 0.925 | 0.160 | +1.83 | 0 | | |
| Chiral | $0.0(\tilde{M}^*=.851)$ | | | 244 | 1.61 | 1.05 |
| $\sigma$-Model[5] | $0.0(\tilde{M}^*=.824)$ | | | 358 | 1.61 | 0.78 |
| Paris[16] | 0.0 | 1.000 | −18.35 | $182\pm9$ | 2.03 | 1.12 |
| ($\rho_0=.289$ fm$^{-3}$) | 0.2 | 0.962 | −16.74 | $174\pm6$ | | |
| | 0.4 | 0.823 | −12.19 | $127\pm9$ | | |
| SIII[29] | 0.0 | | | 355 | 1.28 | |
| ($\rho_0=.145$ fm$^{-3}$) | 0.33 | | | 306 | | |
| SKM*(HF)[29] | 0.0 | | −15.77 | 217 | 1.60 | |
| ($\tilde{M}^*=.795$) | 0.33 | | | 179 | | |
| SKM*(TF)[28] | 0.0 | | | 217 | 2.00 | 0.75 |
| | 0.33 | | | 170 | | |
| AV14+UVII[18] | 0.0 | | −12.4 | 209 | 2.196 | |
| ($\rho_0=.194$ fm$^{-3}$) | 0.33 | | | 159 | | |

approach for their calculations. Das et al.[3] who used non-relativistic Brueckner theory observed that the above relation is valid for temperature up to $T = 20$ MeV. We have plotted the difference $[B(\rho,T,\beta) - B(\rho,T,\beta = 0)]$ against $\beta^2$ in Fig. 2 for $T = 0$, 20 and 40 MeV for $\rho_B/\rho_0 = 1/2$, 1, 2 and 5 in the case when the model is characterized by $\alpha = 1/4$. Values of $B(\rho_B, T = 0, \beta)$ have also been listed in Table I for several values of $\beta$ and $\alpha$. In every case the above parabolic law has been found to be fairly correct. We also find that as the value of the asymmetry parameter $\beta$ increases the minimum in the binding energy versus density curve gradually disappears before pure neutron matter ($\beta = 1$) is reached as can be seen from Table I. This is due to the fact that as $\beta$ increases the system becomes more and more unbound.[2] It is found that $(\epsilon/\rho - M)$ and pressure $P$ both vanish at $\beta_{fl}$ given by $\beta_{fl} = 0.79(0.562\rho_0)$, $0.82(0.415\rho_0)$ and $0.84(0.32\rho_0)$ for $\alpha = 0, 1/4$ and 1, respectively. The quantities within the parenthesis refer to the corresponding density.

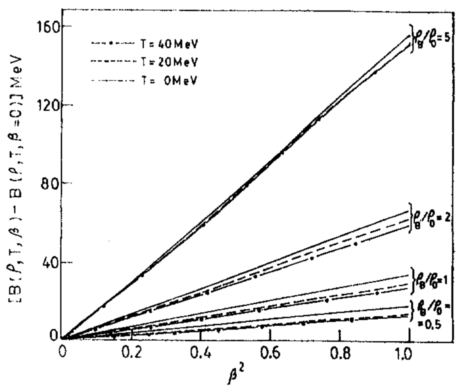


Fig. 2. Variation of $[B(\rho_B,T,\beta) - B(\rho_B,T,\beta = 0)]$ with $\beta^2$ for different densities and temperatures for $\alpha = 1/4$.

### 3.2. *Symmetry energy*

In view of the parabolic law for binding energy expressed by Eq. (30), the symmetry energy $E_{\rm sym}(\rho_B,T)$ can be written as[16]

$$E_{\rm sym}(\rho_B,T) = \frac{1}{2}\frac{\partial^2 B}{\partial \beta^2}\bigg|_{\beta=0}, \qquad (32)$$

$E_{\rm sym}(\rho_B,T)$ can also be determined from the two extreme situations of pure neutron matter ($\beta = 1$) and symmetric nuclear matter ($\beta = 0$) by using the following formula,

$$\begin{aligned} E_{\rm sym}(\rho_B,T) &= B(\rho_B,T,\beta=1) - B(\rho_B,T,\beta=0) \\ &= E(\rho_B,T,\beta=1) - E(\rho_B,T,\beta=0). \end{aligned} \qquad (33)$$

We have calculated the symmetry energy $E_{\rm sym}(\rho_B,T)$ at different temperatures and densities by using Eq. (33). The symmetry energy at a particular temperature and density can also be obtained from the corresponding line shown in Fig. 2. Using nonrelativistic Brueckner theory with effective interaction Das et al.[3] have studied variation of $E_{\rm sym}(\rho_B,T)$ with $\rho_B$ for $T = 10$ and 20 MeV. Somewhat similar work has been

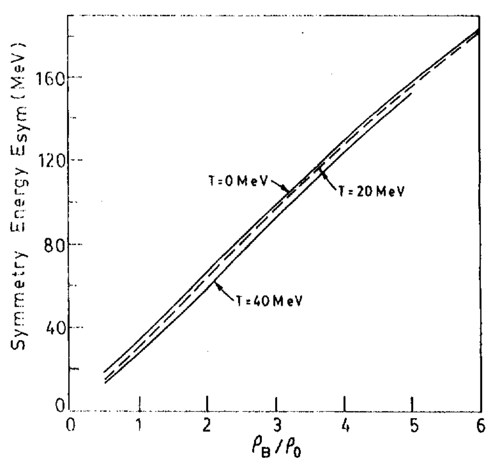


Fig. 3. Symmetry energy versus density at $T = 0$ MeV, 20 MeV and 40 MeV for $\alpha = 1/4$.

done by Bombaci and Lombardo[16] for zero temperature. In Fig. 3 we have plotted symmetry energy $E_{\rm sym}(\rho_B, T)$ against density for $T = 0$, 20 and 40 MeV for our relativistic field theoretic model characterized by $\alpha = \frac{1}{4}$. In our calculation the value of the symmetry energy at saturation density for $T = 0$ is found to be 34 MeV which is in good agreement with the empirical value taken from the mass formula.[24] The value of $C_\rho^2$ defined by (24) is calculated by using the following formula,[12]

$$C_\rho^2 = \left[E_{\rm sym}(\rho_B = \rho_0, T = 0) - \frac{1}{6}\frac{k_F^2}{(k_F^2 + M^{*2})^{1/2}}\right]\frac{12\pi^2 M^2}{k_F^3}, \qquad (34)$$

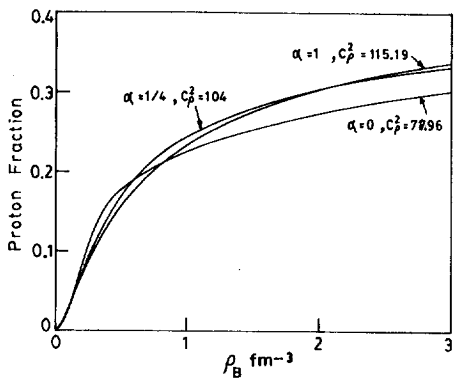


Fig. 4. Proton fraction against density for different values of $\alpha$ and corresponding $C_\rho^2$ as given in Table II.

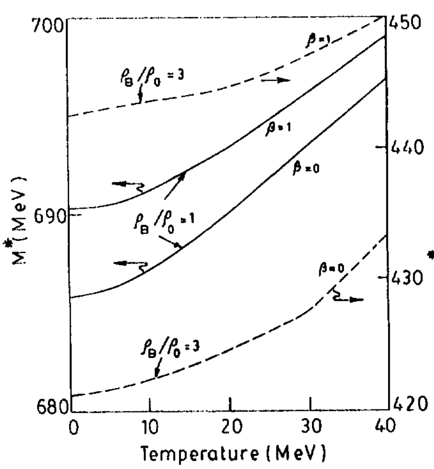


Fig. 5. Variation of effective mass of symmetric nuclear matter ($\beta = 0$) and pure neutron matter ($\beta = 1$) with temperature for $\rho_B/\rho_0 = 1$ and 3 for $\alpha = 1/4$. The scale for $M^*$ in the case $\rho_B/\rho_0 = 1$ (solid lines) is given on the left side and that for the case with $\rho_B/\rho_0 = 3$ (dashed lines) is written on the right side.

where $E_{\rm sym}(\rho_B = \rho_0, T = 0) = 34$ MeV and $k_F$ is the saturation Fermi momentum of symmetric nuclear matter ($k_{F_p} = k_{F_n} = k_F$). It is found from Fig. 3 that the symmetry energy increases with density for a particular temperature. Figure 3 further shows that $E_{\rm sym}(\rho_B, T)$ decreases with temperature at a fixed density. This may be due to the fact that $M^*$ (appearing in (34)) increases with $T$ in the low temperature region as can be seen from Fig. 5. In Table II we have given the values of $C_\rho^2$ for different values of $\alpha$ (related to bulk modulus $K$). It can be seen that $C_\rho^2$ increases with increasing $\alpha$ which is due to the fact that $M^*$ (at saturation density) appearing in (34) increases with $\alpha$.

It may be pointed out that symmetry energy of an asymmetric system in a certain way determines the amount of possible beta decay of some of the neutrons near the top of Fermi sea.[5] Bombaci and Lombardo[16] have shown that in neutron rich star ($\beta \cong 1$) the proton fraction

$$Y = 1/2(1 - \beta) = Z/(N + Z) \quad (35)$$

at zero temperature is approximately given by

$$Y \cong 1/2(4E_{\rm sym}/k_F)^3 \qquad (36)$$

which is obtained by minimizing the internal energy. It follows from Eqs. (34)

Table II. Values of the coupling constants to obtain the saturation nuclear matter properties (binding energy = −16 MeV, Fermi momentum $k_F = 1.33$ fm$^{-1}$, symmetry energy = 34 MeV) for different values of the hybridization parameter $\alpha$.

| $\alpha$ | $\tilde{M}^*$ | $C_s^2$ | $C_v^2$ | $C_\rho^2$ | $K$(MeV) |
|---|---|---|---|---|---|
| 0.0 | 0.54 | 357.4 | 273.8 | 77.0 | 548 |
| 0.25 | 0.73 | 235.0 | 136.0 | 104 | 307 |
| 0.5 | 0.79 | 192.2 | 92.87 | 109.9 | 265 |
| 0.75 | 0.82 | 180.0 | 73.0 | 112.6 | 239 |
| 1.0 | 0.85 | 169.5 | 59.1 | 115.0 | 225 |

and (36) that proton fraction increases with density as shown in Fig. 4. Bombaci and Lombardo[16] have remarked that in the final stage of a pre-supernova collapse electron capture process leads to an equilibrium state where $\beta$ and proton fraction are about 1/3. They further observed that this proton fraction is controlled by symmetry energy.

For non-zero temperature ($T \neq 0$) proton fraction ($Y$) is obtained by minimizing the free energy per baryon, $F = (\epsilon - Ts)/\rho$ with respect to $Y$. In the following we construct an expression for $Y$ in the region of low temperature and density around normal nuclear matter density.

Using the results of Fermi integral and some previous results[25] we obtain the expressions for the density $\rho_i$ defined by (7) and other thermodynamic quantities like energy density $\epsilon_i$ given by (18) and $P_{Fi}$ defined by Fermi integral part of (19).

$$\rho_i = \frac{\gamma_i}{2\pi^2}\left[\frac{1}{3}(\nu_i^2 - M^{*2})^{3/2} + \zeta(2)T^2\frac{2\nu_i^2 - M^{*2}}{(\nu_i^2 - M^{*2})^{1/2}} + \cdots\right] = \frac{\gamma_i}{6\pi^2}k_{Fi}^3(\text{say}), \tag{37}$$

where $\zeta(2) = \pi^2/6$ and the suffix $i$ stands either for neutron or proton. We have

$$k_{F_{p,n}} = (1 \mp \beta)^{1/3}k_F, \tag{38}$$

using Eqs. (18), (19), (37) and (38) we find[25]

$$\epsilon_i = \epsilon_{i,T=0} + \frac{\pi^2}{2}\rho_i\frac{M^*}{k_{Fi}^2}T^2 + \cdots \tag{39}$$

and

$$P_{Fi} = P_{Fi,T=0} + \frac{\pi^2}{3}\rho_i\frac{M^*}{k_{Fi}^2}T^2 + \cdots. \tag{40}$$

Using standard relations and Eqs. (25), (26) and (37)∼(40), we obtain the following expression for entropy density $s_i$,

$$Ts_i = \epsilon_i + P_i - \mu_i\rho_i = \pi^2\rho_i\frac{M^*}{k_{Fi}^2}T^2 + \cdots. \tag{41}$$

In view of the above relations the free energy $F = E - Ts = -P + \mu\rho$ for hadrons is given by

$$(F/\rho)_h = (F/\rho)_{h,\beta=0} + \beta^2\left[E_{\text{sym}} + \frac{\pi^2}{18}M^*\frac{T^2}{k_F^2}\right]. \tag{42}$$

In beta equilibrium mass of the electron may be neglected, energy density[26] at low temperature can be expressed by the relation

$$\epsilon_l = 3P_l = 1/(\pi^2)\left[\frac{1}{4}\nu_l^4 + 3\zeta(2)T^2\nu_l^2 + \cdots\right] \tag{43}$$

applying Eqs. (37), (41) and (43) we obtain

$$(F/\rho)_l = \frac{3}{8}\left[k_F(2Y)^{4/3} - \frac{4}{k_F}T^2(2Y)^{2/3}\right]. \tag{44}$$

The suffixes $h$ and $l$ in (42) and (44) refer to hadrons and leptons or electrons, respectively. Using the procedure of Bombaci and Lombardo,[16] we obtain from (42), (44) and (35) the following relations to determine proton fraction $Y$,

$$4\left[E_{\rm sym} + \frac{\pi^2}{18}M^*\left(\frac{T}{k_F}\right)^2\right] = k_F(2Y)^{1/3}\left[1 - 2\zeta(2)\left(\frac{T}{k_F}\right)^2(2Y)^{-2/3}\right] \tag{45}$$

or

$$Y^{1/3} \cong \frac{4E_{\rm sym}}{2^{1/3}k_F}\left[1 + \pi^2\left(\frac{T}{k_F}\right)^2\left(\frac{1}{18}\frac{M^*}{E_{\rm sym}} + \frac{1}{3}\left(\frac{k_F}{4E_{\rm sym}}\right)^2\right)\right]. \tag{46}$$

Expression (46) shows that proton fraction $Y$ increases with increasing temperature.

### 3.3. *Effective mass*

It is of interest to study the nature of the variation of effective nucleon mass $M^*$ with temperature $T$ for different normalized densities $\rho_B/\rho_0$ (= 1 and 3) in the case of symmetric matter ($\beta = 0$) and neutron matter ($\beta = 1$). Curves for the above cases with $\alpha = 1/4$ are plotted in Fig. 5. It is found that $M^*$ increases with temperature and also with asymmetry parameter $\beta$ while it decreases with $\rho_B/\rho_0$. However, $M^*$ decreases with $T$ when temperature is very large. For a particular $\rho_B/\rho_0$ difference between the values of $M^*$ for $\beta = 0$ and that for $\beta = 1$, slowly decreases with increasing $T$. Further, $\beta$ dependence of $M^*$ is decreased when $\rho_B/\rho_0$ is diminished. We may mention that using modified Sussex interaction and Brueckner method Das et al.[27] have discussed the variation of $M^*$ for nuclear matter and neutron matter with temperature. Nishizaki et al.[15] have also studied $\beta$, $T$ and density dependence of effective proton and neutron masses in the framework of temperature dependent Hartree-Fock theory with an effective interaction.

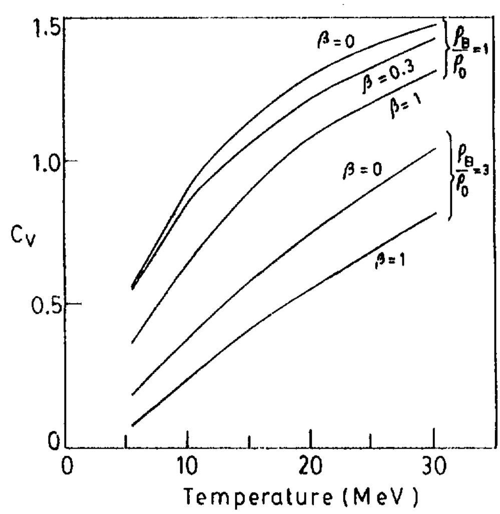


Fig. 6. Specific heat $C_v$ is plotted against temperature $T$ for different values of $\beta$ and for $\rho_B/\rho_0 = 1$ and 3 for $\alpha = 1/4$.

### 3.4. *Specific heat*

In Fig. 6 we have plotted specific heat per nucleon at constant volume $C_V$ (for $\alpha = 1/4$) with temperature for $\beta = 0$ (symmetric nuclear matter) and $\beta = 1$ (neutron matter) with $\rho_B/\rho_0 = 1$ and 3. A similar curve for asymmetric nuclear matter with $\beta = 0.3$ at $\rho_B/\rho_0 = 1$ is also displayed in the above figure. The reason for the decrease of $C_V$ with increased $\beta$, as shown in Fig. 6, lies in the fact that at a certain density the thermal effect is stronger for symmetric nuclear matter than that for neutron matter involving different Fermi momenta.[15] Further $C_V$ is larger for smaller $\rho_B/\rho_0$ since thermal effect is enhanced for lower density. Figure 6 also displays that the variation of $C_V$ with $T$ is more linear for larger $\rho_B/\rho_0$.

### 3.5. *Bulk modulus*

The nuclear matter compressibility $K$ (or the bulk modulus) is a very significant quantity to characterize the nuclear medium. A correct determination of this quantity is required for the study of heavy ion reaction, pre-supernova collapse and neutron star. As mentioned in §1 'conflicting constraint' on the value of $K$ arising from supernova dynamics and maximum neutron star mass[15] can possibly be resolved by considering asymmetry and temperature dependence of $K$. So it is of interest to investigate how the nuclear matter compressibility changes with asymmetry parameter $\beta$, temperature $T$ and also with hybridization parameter $\alpha$. We have evaluated bulk modulus for particular values of temperature $T$ and asymmetry parameter $\beta$ using the following relation,

$$K(\rho_B, \beta, T) = 9(\partial P/\partial \rho_B)\Big|_{\rho_B=\rho_0(T,\beta)}, \tag{47}$$

where $\rho_0(T, \beta)$ is the saturation density at temperature $T$ and asymmetry parameter $\beta$ for which pressure vanishes. In our calculation it is found that the compressibility $K$ decreases as the temperature $T$ increases for a particular value of $\beta$ and $K$ vanishes at a certain temperature, called flashing temperature $T_{fl}$. In Fig. 7 we have shown the variation of $K$ ($\beta = 0, T$) with temperature $T$ for symmetric nuclear matter ($\beta = 0$) for different values of hybridization parameter $\alpha$. From Fig. 7 it is further found that the flashing temperature $T_{fl}$ falls off with increasing $\alpha$ (or decreasing $K$ associated with $\alpha$). This variation of bulk modulus with temperature $T$ can be fitted well with the following parabolic law,[2]

$$K(\beta, T) = K(\beta, T = 0)(1 - a_T(\beta)T^2). \tag{48}$$

It appears from Fig. 7 that '$a_T$' decreases as the value of the hybridization parameter $\alpha$ increases. Further, Table III shows that $a_T$ increases as $\beta$ is enhanced from 0 to 0.3 for temperature $T$

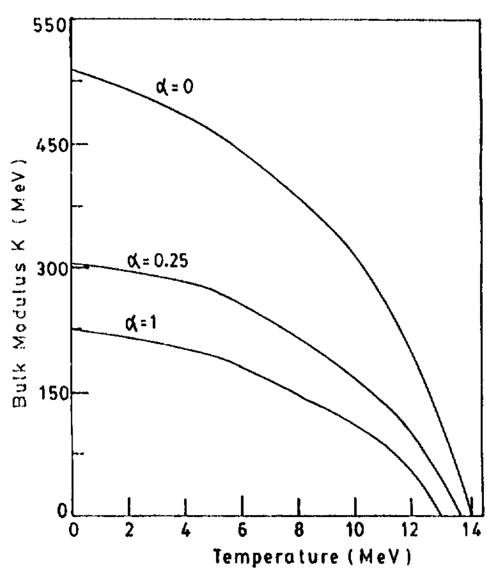


Fig. 7. Bulk modulus $K$ is plotted against temperature $T$ for symmetric nuclear matter ($\beta = 0$) for different values of $\alpha$.

Table III. Dependence of the bulk quantities like saturation density $\rho_0(\beta, T)$, bulk modulus $K$, parameter $a_T(\beta)$ (defined by (48)), entropy per nucleon $s/\rho$ and iso-entropic compressibility $K_s$ on asymmetry parameter $\beta$ and temperature $T$ for different models.

| Model | $\beta$ | $T$ MeV | $\frac{\rho_0(\beta,T)}{\rho_0}$ | $K$ MeV | $a_T(\beta)$ $10^{-3}$ MeV$^{-2}$ | $s/\rho$ | $K_s$ MeV |
|---|---|---|---|---|---|---|---|
| | 0 | 0 | 1.0 | 307 | 5.1 | | |
| | | 4 | 0.977 | 287 | | | |
| | | 6 | 0.945 | 255 | | | |
| $\alpha = 0.25$ | | 8 | 0.905 | 222 | | | |
| | | 10 | 0.84 | 168 | | 1.15 | 239 |
| | | 12 | 0.747 | 103 | | 1.45 | 188 |
| | | 13 | 0.673 | 59 | | 1.65 | 158 |
| | 0.3 | 0 | 0.917 | 272 | 6.8 | | |
| | | 5 | 0.86 | 225 | | | |
| $\alpha = 0.25$ | | 10 | 0.78 | 87 | | | |
| | | 11 | 0.67 | 55 | | | |
| | | 12 | 0.62 | 39 | | | |
| Paris[16] | 0.33 | 0 | | 144 | 7.87 | | |
| ($\rho_0 = .289$ | | 4 | | 131 | | | |
| fm$^{-3}$, | | 6 | | 101 | | | |
| $B = -18.35$ | | 8 | | 71.4 | | 0.5 | 134 |
| MeV) | | | | | | 1.0 | 99 |
| | | | | | | 1.5 | 34 |
| SKM*(HF)[28] | 0.33 | 0 | | 179 | 7.33 | | |
| ($\tilde{M}^* = .795$) | | 4 | | 158 | | | |
| | | 6 | | 129 | | | |
| | | 8 | | 89 | | | |
| | | 10 | | 29 | | | |

to be quite small ($\leq$ 12 MeV). Values of '$a_T$' and $K$ $(\beta, T)$ for different values of $\beta$ (0 and 0.3) and $T$ are given in Table III for the model characterized by $\alpha = 1/4$. Table III also displays values of $K$ $(\beta = .33, T)$ determined by several authors[2] who used interaction potential approach in the framework of Brueckner-Bethe-Goldstone theory and other investigators[28),29] who performed Hartree-Fock calculation with different Skyrme type interaction SKM* $(HF)$ and SKM* $(TF)$.

The nuclear matter compressibility is always found to decrease with the increase in asymmetry parameter $\beta$. This decrease in $K$ can be described by the following relation,[13),2]

$$K(\beta, T = 0) = K(0,0)(1 - a\beta^2). \tag{49}$$

From field theoretic formulation

$$a = \frac{9}{K}\left[\frac{9P_\beta}{K}\frac{d^2\overline{P}}{d\rho^2} - \frac{dP_\beta}{d\rho}\right]\Bigg|_{\rho=\rho_0}, \tag{50}$$

where pressure $P$ is given by

$$P = \overline{P} + \beta^2 P_\beta, \tag{51}$$

where $P$ stands for pressure due to symmetric matter ($\beta = 0$) and

$$P_\beta = \rho^2 dE_{\rm sym}/d\rho. \tag{52}$$

The relation (50) in a different equivalent form has been given by other investigators.[5] In Table I values of '$a$' for models based on two-body and three-body interaction potentials[16),29),28] and field theoretic models like hybrid derivative coupling model (for $\alpha = 0, 1/4$ and 1) and chiral sigma model[5] are listed. It may be noted that in chiral sigma model, effective nucleon masses $M^*/M = 0.851$ and 0.824, corresponding to $K = 244$ MeV and 358 MeV, respectively, are quite large in comparison with the recent empirical value for $M^*/M = 0.69$.[30]

The relation (49) holds quite well for small value of $\beta$. Using the above-mentioned models values of $K(\beta, T = 0)$ for several values of asymmetry parameter $\beta$ are given in Table I. Further, values of $\beta = \beta_{infl}$ and other related quantities for which both pressure and $K(\beta_{infl}, T = 0)$ vanish are reported in Table I for $\alpha = 0, 1/4$ and 1. The above-mentioned results show that bulk modulus $K$ decreases as the value of the asymmetry parameter $\beta$ or the temperature $T$ increases. This implies that the EOS becomes softer as $\beta$ or $T$ increases. This soft EOS is found to be very useful in understanding the generation of strong shock wave[5] initiated by rebounding core in a stellar collapse and the mechanism of subsequent explosion of type II supernova.[16] This decrease in the value of compressibility as $\beta$ or $T$ increases is due to the fact that with the increase in $\beta$ or $T$ the system becomes less and less bound and the saturation density shifts to some lower value. This decrease in the value of the saturation density $\rho_0(\beta, T)$ with $\beta$ and $T$ can be fitted approximately by the following relations,[2]

$$\rho_0(\beta) = \rho_0(\beta = 0)(1 - b\beta^2) \tag{53}$$

and

$$\rho_0(\beta, T) = \rho_0(\beta, T = 0)(1 - b_T(\beta)T^2), \tag{54}$$

where for field theoretic model $b = (9\rho_0/K)d/d\rho(E_{\rm sym})$ as given by several authors.[5] Equation (54) holds quite well for small value of $T$. In Table I we list values of the parameters $a$ and $b$ for hybrid derivative coupling model (for $\alpha = 0, 1/4$ and 1), chiral sigma model[5] and various types of Skyrme interaction.[28),29] Values of $b_T(\beta)$ defined by (54) are found to be $b_T(0) = 1.65 \cdot 10^{-3}$ MeV$^{-2}$ for $\beta = 0$, $\alpha = 1/4$ and $b_T(.3) = 2.04 \cdot 10^{-3}$ MeV$^{-2}$ for $\beta = 0.3$ and $\alpha = 1/4$ which implies an increase of $b_T(\beta)$ with $\beta$. Isoentropic bulk modulus $K_s$, for different values of entropy per nucleon with $\alpha = 1/4$ (in our model) and also similar results of Bombaci et al.[2] are listed in Table III. It is found that $K_s$ decreases as entropy per nucleon $(s/\rho)$ increases. As expected, the isoentropic bulk modulus $K_s$ is found to be greater than the corresponding isothermal bulk modulus which can be seen from Table III in the case $\alpha = 0.25$ and $\beta = 0$.

We have compared our results for the parameters which govern the variation of compressibility, saturation density, binding energy and isoentropic compressibility with asymmetry parameter $\beta$ and/or temperature $T$ with the existing results of recent investigators. Some of the bulk properties like saturation density $\rho_0$, binding energy $B$, compressibility $K$ and effective mass $M^*$ at saturation obtained by several investigators as shown in Tables I and III do not agree very well with the empirical values where as the corresponding results of our model (characterized by hybridization parameter $\alpha = 1/4$) are quite satisfactory. So it is likely that the numerical values of the above-mentioned characteristics of nuclear matter in our model are somewhat more acceptable than the corresponding results obtained by other investigators. It may be seen from Tables I and III that $\rho_0 = 0.284\ \text{fm}^{-3}$, binding energy $B = -18.35$ MeV and $K = 182 \pm 9$ MeV in Bombaci et al.'s work[16] based on Paris potential and effective mass $M^* = 0.85\ M$ appearing in the investigation of Prakash and Anisworth[5] based on chiral $\sigma$ model, differ much from the corresponding empirical values of the bulk properties when we keep in mind the recent estimates of Jaminon and Mahaux[30] for $M^* = 0.69\ M$ and Sharma et al.'s[31] estimate of $K$ to be $300 \pm 25$ MeV. Some of the above investigators used a combination of two-nucleon potential based on nucleon-nucleon scattering data and a phenomenological three-body potential adjusted to give correct energies for light nuclei and improved nuclear matter properties at saturation. Our relativistic field theoretic model is likely to give better results for properties of high density asymmetric nuclear matter than the nonrelativistic potential formalism of these investigators.

### 3.6. *Chemical potential*

The chemical potentials of neutron and proton at zero and finite temperatures are evaluated using the relations (25) and (26). The asymmetry ($\beta$) dependence of chemical potential is shown in Fig. 8 for $\rho_B = \rho_0$ and $\rho_B = 3\rho_0$ at $T = 0$ and 25 MeV. It is found that as the value of the asymmetry parameter ($\beta$) increases, the chemical potential of neutron, $\mu_n$, increases and that of proton, $\mu_p$, decreases. As expected both $\mu_n$ and $\mu_p$ are found to increase with the increase in baryon density $\rho_B$. They further decrease slightly as the temperature $T$ increases. It is evident from Fig. 8 that thermal effect in chemical potential decreases as density increases as in the case of $(\epsilon/\rho - M)$ (see Fig. 1). Somewhat similar results are obtained by Nishizaki et al.[15] who used the temperature dependent Hartree-Fock theory with an effective interaction. Das et al.[27] have also studied the temperature and density dependence of chemical potential for symmetric nuclear matter ($\beta = 0$) and neutron matter ($\beta = 1$). Further, Das et al.[27] have plotted $(\mu_n - \mu_p)$ against density. From Fig. 8 we can also extract $(\mu_n - \mu_p)$ for any value of $\beta$ when $\rho_B = \rho_0$ and $\rho_B = 3\rho_0$. It may be pointed out that in beta stable neutron rich matter the relation $(\mu_n - \mu_p) = \mu_e(\mu_e = k_{F_p}$ being the chemical potential of electron) controls the proton fraction in beta equilibrium state of neutron rich matter.

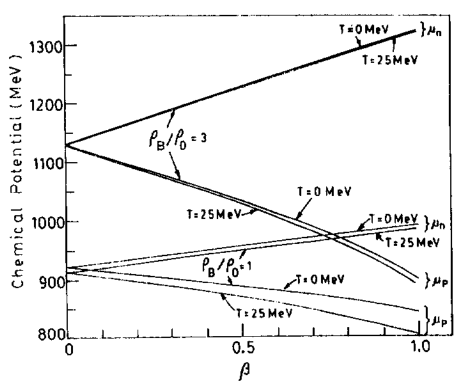


Fig. 8. Chemical potentials of neutron ($\mu_n$) and proton ($\mu_p$) as function of the asymmetry parameter $\beta$ with $\rho_B = \rho_0$ and $3\rho_0$ at two different temperatures $T = 0$ MeV and 25 MeV for $\alpha = 1/4$.

### 3.7. *Entropy*

We have calculated the entropy per nucleon which remains constant during adiabatic process by using Eq. (28). In Fig. 9 entropy per nucleon has been plotted against normalized density $\rho_B/\rho_0$ for $\beta = 0, 0.3$ and 1 at temperatures $T = 20$ and 40 MeV. Figure 9 shows that entropy per nucleon ($s/\rho$) increases as the nucleon density decreases which may be related to the fact that the thermal effect is larger in the low density region.[15] This can also be understood from Eq. (41). As the asymmetry parameter $\beta$ increases the entropy decreases and which can also be explained with the help of relations (41) and (38). For pure neutron matter ($\beta = 1$) the entropy decreases by about 25 % compared to that for symmetric matter ($\beta = 0$) in our field theoretic model. Somewhat similar results have been observed by other authors.[15] We have found numerically that $s/\rho$ at $T = 20$ MeV is almost two times the corresponding result for $T = 10$ MeV. Such results have also been obtained by Nishizaki et al.[15] It can be seen from Fig. 9 and actual numerical calculation that at some higher temperature like $T = 40$ MeV, entropy per nucleon is somewhat less than two times the corresponding value at $T = 20$ MeV implying some deviation from linear dependence of $s/\rho$ on $T$ at higher temperature. Jacak et al.[17] measured the entropy per nucleon from the fragment distributions of the heavy-ion reaction using $^{40}$Ar beams of 42, 92 and 137 MeV/nucleon and Au target. They obtained $s/\rho \cong 2 - 2.4$ at temperature $T \cong 18$, 25 and 35 MeV and the corresponding density lies in the range of $(0.3 - 0.7)\rho_0$. In our calculation we have found $s/\rho = 2.14$ at $T = 20$ MeV for symmetric nuclear matter ($\beta = 0$) with $\rho_B = 0.72\rho_0$.

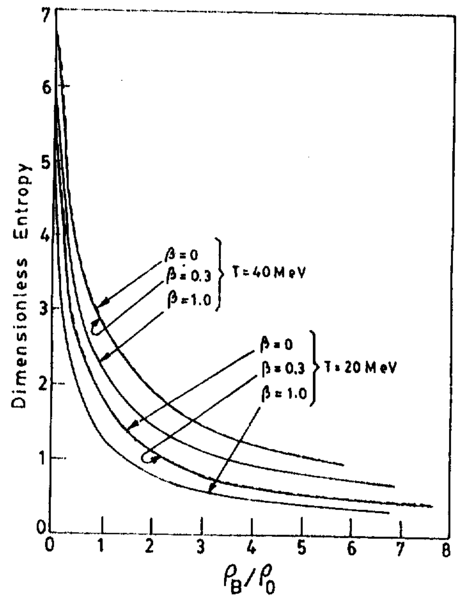


Fig. 9. Entropy per nucleon $s/\rho$ as function of dimensionless density $\rho_B/\rho_0$ for $\beta = 0.0, 0.3$ and 1.0 at temperatures $T = 20$ MeV and 40 MeV for $\alpha = 1/4$.

### 3.8. *Liquid gas phase transition*

The pressure versus density curves at several temperatures are displayed in Fig. 10 for $\beta = 0$, 1/3 and 1 in the region of low density and low temperatures. They exhibit some features signifying liquid gas phase transition as in the case of a non-ideal gas with van der Waals type interaction. This first order liquid gas phase transition in nuclear matter occurs at sufficiently low density $\rho_B < \frac{1}{2}\rho_0$ and below some critical temperature $T_c$ ($< 20$ MeV). In this paper we have studied the asymmetry dependence of the characteristics of liquid gas phase transition like critical temperature $T_c$ and the corresponding pressure $P_c$ and normalized density $\rho_c/\rho_0$ for $\alpha = 1/4$. These quantities also depend upon the value of the hybridization parameter $\alpha$.

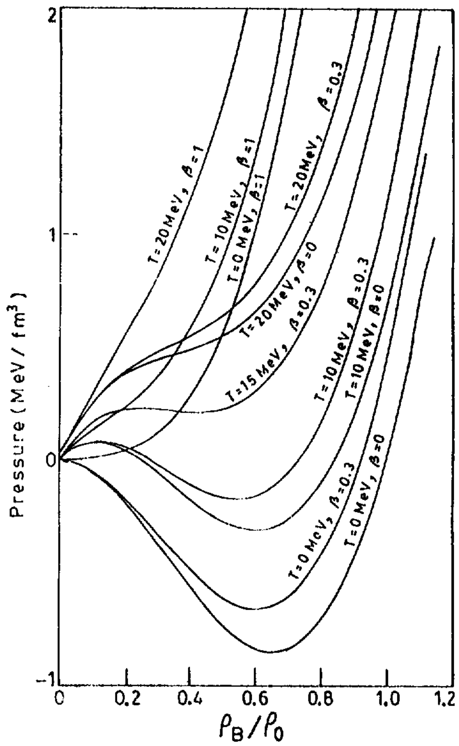


Fig. 10. Equation of state where pressure $P$ is plotted against dimensionless density $\rho_B/\rho_0$ for $\beta = 0.0, 0.3$ and 1.0 and for temperatures $T = 0, 5$ and 15 MeV for $\alpha = 1/4$.

It appears from Fig. 10 that as the asymmetry parameter $\beta$ increases the coexistence region of the two phases becomes narrower and the critical temperature $T_c$ decreases and finally becomes zero before pure neutron matter ($\beta = 1$) is reached, indicating absence of liquid gas phase transition. In our model it is found that $T_c$ and other related quantities are diminished as hybridization parameter $\alpha$ is enhanced (or bulk modulus is diminished) as observed by other investigators.[32] In our calculation for the model characterized by $\alpha = \frac{1}{4}$ we find that the liquid gas phase transition disappears for $\beta > 0.85$ and for $T > 17.5$ MeV. In Table IV we have listed the values of critical temperature $T_c$ and related quanitities $\rho_c/\rho_0$ and $P_c$ for different values of $\beta$ for the model characterized by $\alpha = 1/4$. Results of Nishizaki et al.[15] for $T_c$ for different values of $\beta$ are also reported in the table.

Table IV. Characteristics of liquid gas phase transition for different values of asymmetry parameter.

| Model | $\beta$ | $T_c$ MeV | $\rho_c/\rho_0$ | $P_c$ MeV/fm$^3$ |
|---|---|---|---|---|
| $\alpha = 1/4$ | 0.0 | 17.5 | 0.357 | 0.313 |
| ($K = 307$ | 0.3 | 16.0 | 0.310 | 0.273 |
| MeV) | 0.6 | 11.5 | 0.270 | 0.162 |
| | 0.7 | 9.00 | 0.250 | 0.105 |
| Nishizaki | 0.0 | 18.5 | | |
| et al.[15] | 0.2 | 18.0 | | |
| ($K = 250$ MeV) | 0.4 | 16.0 | | |
| | 0.6 | 13.0 | | |

## §4. Summary

We have studied the dependence of the properties of asymmetric nuclear matter on temperature $T$, and asymmetry parameter $\beta$ in the framework of generalized hybrid derivative coupling model.[6] The asymmetry dependence of the bulk properties in field theoretic model can be explained by the presence of interaction term involving vector-isovector meson and is also due to different Fermi momenta possessed by neutron and proton. The thermal effect on the bulk quantities is larger in the low density region than in the high density region. Both the quantity $[B(\rho, T, \beta) - B(\rho, T, \beta = 0)]$ and the symmetry energy $E_{\rm sym}(\rho_B, T)$ increase with density and decrease with temperature. The empirical parabolic law satisfied by the binding energy per nucleon is confirmed by the present calculation in all the range of asymmetry parameter and also for high density ($\geq 5\rho_0$) and high temperature ($\geq 40$ MeV). The EOS becomes softer as the value of asymmetry parameter $\beta$ or temperature $T$ increases. This helps us to understand the dynamics of supernova 'implosion-explosion'.[4] The saturation density shifts to some lower value as $\beta$ or $T$ increases. In our model we can have a soft or stiff EOS depending upon the value of hybridization parameter $\alpha$. The chemical potential of neutron, $\mu_n$, increases and that of proton, $\mu_p$, decreases with $\beta$. Both $\mu_p$ and $\mu_n$ increase with density and decrease with temperature. We may mention that symmetry energy $E_{\rm sym}$ and also the difference $(\mu_n - \mu_p)$ controls the proton fraction of neutron rich matter in beta equilibrium. Adiabatic processes are characterized by constant entropy per nucleon which increases with the increase of temperature and decreases as density or asymmetry parameter $\beta$ increases. The characteristics $(T_c, P_c, \rho_c)$ of liquid gas phase transition are strongly asymmetry parameter dependent. As the value of asymmetry parameter increases the coexistence region becomes narrower and the critical temperature decreases. Finally, for asymmetry parameter close to unity or for pure neutron matter the critical temperature vanishes indicating the absence of liquid gas phase transition.

## References


1) H. A. Bethe, Rev. Mod. Phys. **62** (1990), 801.
2) I. Bombaci, T. S. Kuo and U. Lombardo, Phys. Rep. **242** (1994), 165 and references therein.
3) C. Das, R. Sahu and B. K. Tripathi, Phys. Rev. **C48** (1993), 1056.
4) B. ter Haar and Rudi Malflied, Phys. Rev. Lett. **59** (1987), 1652.
5) M. Prakash and T. L. Ainsworth, Phys. Rev. **C36** (1987), 346.
6) S. Sarkar and B. Malakar, Phys. Rev. **C50** (1994), 757.
7) R. Rakshit and S. K. Choudhury, Phys. Rev. **C53** (1996), 505.
8) J. Zimanyi and S. A. Moszkowski, Phys. Rev. **C42** (1990), 1416.
9) A. Delfino, C. J. Coelho and M. Malheiro, Phys. Lett. **B345** (1995), 361.
10) K. Miyazaki, Prog. Theor. Phys. **93** (1995), 137.
11) J. D. Walecka, Ann. of Phys. **83** (1974), 491.
B. D. Serot and J. D. Walecka, Adv. in Nucl. Phys. Vol. 16, ed. J. W. Negele and E. Vogt (Plenum, New York, 1986).
12) N. K. Glendenning, F. Weber and S. A. Moszkowski, Phys. Rev. **C45** (1992), 844.
13) E. Baron, J. Cooperstein and S. Kahana, Phys. Rev. Lett. **55** (1985), 126.
14) R. Stock, Nature **337** (1989), 319.
15) S. Nishizaki, T. Takatsuka and J. Hiura, Prog. Theor. Phys. **92** (1994), 93.
16) I. Bombaci and U. Lombardo, Phys. Rev. **C44** (1991), 1892.
17) B. V. Jacak, G. D. Westfall, C. K. Gelbke, L. H. Harwood, W. G. Lynch, D. K. Scoot, H. Stoker, M. B. Tsang and T. J. M. Symons, Phys. Rev. Lett. **51** (1983), 1846.
18) R. B. Wiringa, V. Fiks and A. Fabrocini, Phys. Rev. **C38** (1988), 1010.
19) M. Brittan, Phys. Lett. **79B** (1978), 27.
20) J. Boguta and A. R. Bodmer, Nucl. Phys. **A292** (1977), 413.
21) S. A. Chin, Ann. of Phys. **108** (1977), 301.
22) M. Barranco, Phys. Rev. **C44** (1991), 178.
23) Jian Kang Zhang and D. S. Onley, Phys. Rev. **C44** (1991), 2230.
24) W. D. Myers, At. Data Nucl. Data Tables **17** (1976), 411.

25) R. K. Pathria, *Statistical Mechanics* (Pergamon Press, 1972), Vol. 45.
26) W. Greiner, L. Neise and H. Stocker, *Thermodynamics and Statistical Mechanics*, (Springer-Verlag, 1994).
27) C. Das, R. K. Tripathi and R. Sahu, Phys. Rev. **C45** (1992), 2217.
28) X. Vinas, M. Barranco, J. Treiner and S. Stringari, Astron. Astrophys. **182** (1987), L34.
29) K. Kolehmainen, M. Prakash, J. M. Lattimer and J. Treiner, Nucl. Phys. **A439** (1985), 535.
30) M. Jaminon and C. Mahaux, Phys. Rev. **C40** (1989), 354.
31) M. M. Sharma, W. T. A. Borghols, S. Brandenburg, S. Crona, A. van der Woude and M. N. Harakeh, Phys. Rev. **C38** (1988), 2562.
32) Zhi-Xin Qian, Hong-Qiu Song and Ru-Keng Su, Phys. Rev. **C48** (1993), 154.